BJ www.biochemj.org

Biochem. J. (2011) **437**, 117–123 (Printed in Great Britain) doi:10.1042/BJ20101898

Identification and characterization of interactions between abscisic acid and mitochondrial adenine nucleotide translocators

Olesya A. KHARENKO*, Jason BOYD*, Ken M. NELSON*, Suzanne R. ABRAMS*† and Michele C. LOEWEN*‡[1]

*Plant Biotechnology Institute, National Research Council of Canada, 110 Gymnasium Place, Saskatoon, SK, Canada S7N 0W9, †Department of Chemistry, University of Saskatchewan, 110 Science Place, Saskatoon, SK, Canada S7N 5C9, and ‡Department of Biochemistry, 107 Wiggins Road, Saskatoon SK, Canada S7N 5E5

ABA (abscisic acid) is a plant hormone involved in important processes including development and stress responses. Recent reports have identified a number of plant ABA receptors and transporters, highlighting novel mechanisms of ABA action. In the present paper we describe application of a chemical proteomics approach leading to the identification of mitochondrial ANTs (adenine nucleotide translocators) as ABA-interacting proteins. Initial *in vitro* studies confirmed inhibition of ANT-dependent ATP translocation by ABA. Further analysis demonstrated ANT-dependent uptake of ABA into both recombinant *Arabidopsis thaliana* ANT2-containing proteoliposomes and native isolated spinach mitochondria; the latter with a K_m of 3.5 μM and a V_{max} of 2.5 nmol/min per g of protein. ATP was found to inhibit ANT-dependent ABA translocation. Specificity profiles highlight the possibility of mechanistic differences in translocation of ABA and ATP. Finally, ABA was shown to stimulate ATPase activity in spinach mitochondrial extracts. ABA concentrations in plant cells are estimated to reach the low micromolar range during stress responses, supporting potential physiological relevance of these *in vitro* findings. Overall, the present *in vitro* work suggests the possibility of as yet uncharacterized mechanisms of ABA action *in planta* related to inhibition of mitochondrial ATP translocation and functional localization of ABA in the mitochondrial matrix.

Key words: abscisic acid, adenine nucleotide translocator, inhibition, mitochondrion, phytohormone, uptake.

INTRODUCTION

ABA (abscisic acid) is a plant hormone known to control many physiological responses, including germination, stomatal opening, desiccation tolerance, seed maturation, dormancy, growth, lateral root formation and modulation of plant responses to environmental stress [1]. This breadth of functionality suggests multiple modulatory mechanisms, a concept that is supported by the increasing number of reports highlighting ABA interacting/receptor proteins. In particular, a family of 14 START domain proteins (RCAR/PYR/PYL) [2,3], two homologous GPCR (G-protein-coupled receptor)-type G-proteins, GTG1 and GTG2 [4], and the magnesium-protoporphyrin IX chelatase large subunit (CHLH) [5] have been shown to function as ABA receptors. These reports demonstrate that ABA signals through both extracellular and intracellular mechanisms, and that these receptors are responsible for mediating at least some of the ABA-associated physiological responses. At the same time, two ABC transport proteins were recently shown to mediate controlled import and export of ABA across cell membranes [6,7]. This highlights a novel mechanism involving protein-catalysed ABA translocation, and emphasizes that passive diffusion of ABA through membranes is probably not the primary mode of ABA translocation [6].

Now, in the present study, through application of a chemical proteomics approach [8,9] mitochondrial ANTs (adenine nucleotide translocators), as well as the F_1-ATP synthase β-subunit are identified as putative ABA-binding proteins. The F_1-ATP synthase β-subunit is one of five subunits (α, β, γ, δ and ε) comprising the matrix-localized F_1 domain of the plant mitochondrial H^+-driven F_1F_O-ATP synthase complex [10,11]. The β-subunit in particular contains the majority of the catalytic site residues comprising the active site where ATP is synthesized from ADP and P_i. ANTs on the other hand contribute to regulation of the rate of ATP synthesis by performing ATP/ADP exchange across the mitochondrial inner membrane [12]. ANTs display a significant flexibility of nucleotide binding, and despite a recent crystal structure (PDB code 1OKC), the mechanism of translocation remains enigmatic [13]. The physiological importance of ANTs is highlighted by the observation that decreases in ANT activity leads to the inhibition of cellular metabolism [14].

The concept of a functional linkage between ABA and mitochondria functionalities is supported by a limited number of other reports. In one instance ABA was shown to protect the mitochondria of maize seedlings from irreversible damage during chilling by inducing expression of antioxidant enzymes [15]. In another report, the gene corresponding to the *Arabidopsis thaliana* (L.) Heynh mitochondrial ANT1 (At3g08580, also known as AAC1) was significantly induced in response to ABA [16]. However, there are other reports linking mitochondrial function to regulation of plant bioenergetics during stress responses [17,18]; and conversely, mitochondrial functionality and related ATP supply have been shown to be affected by abiotic stressors [19–22]. Studies have also implicated roles specifically for some ANTs and ATPases in these stress responses. For example, expression of the gene encoding a mitochondrial 6 kDa ATPase subunit was significantly induced in response to abiotic stress, whereas expression of mitochondrial ATP synthase α- and β-subunits were decreased in response to oxidative stress [23,24]. In another report, activity of the mitochondrial F_1F_O ATPase in aluminium-resistant wheat was induced in response to aluminium stress [25].

These studies linking ABA, stress and mitochondrial function highlight associated mechanisms regulated primarily at the gene expression level. In contrast with this, through applying an

Abbreviations used: ABA, abscisic acid; ANT, adenine nucleotide translocator; DTT, dithiothreitol; ECL, enhanced chemiluminescence; HRP, horseradish peroxidase; LC-MS/MS, liquid chromatography tandem MS.

[1] To whom correspondence should be addressed (email michele.loewen@nrc.ca).

in vitro system that precludes the possibility of regulation by gene expression, in the present study we demonstrate that ABA is transported by mitochondrial ANTs. We show that ABA directly inhibits ANT-mediated ATP translocation and vice versa. We demonstrate unique specificity profiles that highlight the possibility of different binding sites and/or mechanisms of translocation for ABA compared with ATP. Finally we show that ABA can act as an activator of the matrix-localized mitochondrial ATP synthesizing machinery. Taken together the findings of the present study support the novel possibility of functional modulation of mitochondrial proteins by direct interaction with ABA.

EXPERIMENTAL

Materials

All materials were from Sigma–Aldrich unless otherwise indicated. The desalting column (PD-10), HiTrap streptavidin column, streptavidin–HRP (horseradish peroxidase) conjugate, ECL (enhanced chemiluminescence) biotinylated protein markers and ECLplus Western blotting detection reagents and [^{3}H]ABA (DL-*cis*-[G-^{3}H]ABA) were all obtained from Amersham Biosciences. (+)-ABA was prepared as described previously [26]. PBI686, PBI410 and other ABA analogues were synthesized as described by Nyangulu et al. [8,27]. [^{3}H]ATP was obtained from Sigma–Aldrich. All plotted values are means ± S.D, unless otherwise stated.

Preparation of total cell protein extracts from *Brassica napus* cell cultures

The microspore-derived suspension cell culture of *B. napus* L. cv. Jet Neuf was propagated for 2 weeks and maintained on NLN medium containing 6 % sucrose [28,29]. The cultures were induced with 10 μM ABA for 24 h. Freshly harvested cells (100–200 g) were washed with deionized water and homogenized in a blender in the presence of 400–500 ml of ice-cold homogenization buffer [0.33 M sucrose, 40 mM ascorbate, 20 mM EDTA, protease inhibitor cocktail (Complete™, Roche), 0.1 % OG (*n*-octyl-β-D-glucopyranoside; Affymetrix, Santa Clara, CA), 2 mM DTT (dithiothreitol) and 100 mM sodium phosphate buffer (pH 7.5)] and one third of the total volume acid-washed glass beads (500 μm diameter). Homogenates were centrifuged at 1000 ***g*** for 10–15 min, the supernatant was collected and proteins were concentrated by precipitation with 75 % ammonium sulfate at 4 °C. The precipitated proteins were centrifuged at 10000 ***g*** for 15 min and re-dissolved in 10–20 ml of 20 mM phosphate buffer (pH 7.6) containing 6 mM CHAPS. Excess ammonium sulfate was removed by application to a desalting column (PD-10) with buffer-exchange to 20 mM sodium phosphate and 150 mM NaCl (pH 7.5).

Chemical proteomic identification of putative ABA-binding proteins

The resulting protein extract sample was transferred to Pyrex tubes and mixed with 10 μM PBI686, a photoactivable biotinylated ABA mimetic probe [8]. The resulting samples were UV irradiated as described previously [8,9]. Samples treated with UV but no PBI686, or with no PBI686 and no UV were used as negative controls. Tagged proteins were enriched by affinity chromatography using a HiTrap streptavidin column (1–3 ml matrix volume) and the ÄKTA™ Explorer FPLC system. The column was equilibrated with running buffer [20 mM sodium phosphate and 150 mM NaCl (pH 7.5)]. Protein solutions were injected at a flow rate of 0.3 ml/min, washed with the running buffer for 20 column volumes and eluted with a gradient of 8 M guanidine-HCl at pH 2 (1 ml/min, 30 ml in total). Collected fractions were desalted with the PD-10 desalting columns into 20 mM sodium phosphate and 0.15 M NaCl (pH 7.5), and concentrated using Amicon™ Ultrafree centrifugal filters (Millipore). Protein samples were separated by application to SDS/PAGE (10 % gels) according to the method of Laemmli [30]. For Western blot analysis, after gel electrophoresis, the proteins were transferred on to a PVDF membrane for 1 h at 100 V, blocked in PBS-T [PBS (pH 7.5) containing 0.1 % Tween 20] with 3 % (w/v) BSA and further incubated with a streptavidin–HRP conjugate diluted 1:1000 in PBS-T for 1 h at room temperature (22 °C). ECLplus Western blotting detection reagents were applied to the membrane and luminescence was detected using a Storm Scanner (Amersham Biosciences) system. ECL biotinylated protein marker was used as the molecular mass reference.

Alternatively, gels were stained using the FOCUS-FAST silver-stain kit (Genotech) according to the manufacturer's protocol. Protein bands were excised and placed in a 96-well microtitre plate (Sigma). The resulting gel pieces were automatically de-stained, reduced with DTT, alkylated with iodoacetamide and digested with porcine trypsin (sequencing grade; Promega) using a MassPREP protein digest station and recommended procedures (Waters). Peptides from tryptic digestion were analysed using a capLC ternary HPLC system (Waters) coupled to a Q-ToF Ultima Global instrument (Waters). The method used for separation of the peptide digest samples and subsequent analysis using LC-MS/MS (liquid chromatography tandem MS) and DDA (Data Dependent Acquisition) has been described previously [31]. The LC-MS/MS data were processed using ProteinLynx software (Waters) and searched against databases using Mascot Daemon and Mascot MS/MS ion search performed on a Mascot server hosted by IBS (Institute of Biological Sciences)-NRC (National Research Council) (Ottawa, Canada).

Proteoliposome transport assays

Recombinant expression and purification of *A. thaliana* ANT2 (ANT2; At5g13490) was performed as described previously [32]. [^{3}H]ATP transport assays were carried out based on the protocols in Genchi et al. [33], Palmieri et al. [17] and Thuswaldner et al. [34], as described in Kharenko et al. [32], with minor modifications for measurement of uptake of [^{3}H]ABA as follows. Liposomes were preloaded internally with 20 mM (+)-ABA instead of ATP, to ensure that ABA transport would not be influenced by the presence of ATP. Transport was initiated by the addition of 100 nM [^{3}H]ABA. Each experimental point corresponds to the average of six replicates. Externally added substrates (inhibitor, nucleotides and ABA analogues) were added to a final concentration of 200 μM together with ^{3}H-labelled substrate. Transport for these latter experiments was allowed to proceed at room temperature for 10 min and then terminated, with each data point representing the average of four experiments.

Mitochondrial transport assays

Mitochondria were extracted from spinach-leaf as described in Hamasur et al. [35]. Uptake of [^{3}H]ATP or [^{3}H]ABA into mitochondria was characterized using the method described by LaNoue and Schoolwerth [36]. Assays were initiated with the addition of 100 nM [^{3}H]ATP or 188 nM [^{3}H]ABA to spinach mitochondria (50 μg/reaction) and terminated with the addition of the ANT-specific inhibitor pyridoxal 5′-phosphate. Each point represents the average of five replicates. To estimate the kinetic parameters for [^{3}H]ABA uptake, mitochondria were incubated

with increasing concentrations of [^{3}H]ABA (as indicated) and transport was terminated by the addition of pyridoxal 5′-phosphate after 2 min. Each resulting time course curve was fitted to first-order kinetics using Origin software (OriginLab) from which a rate was obtained for the given concentration of ATP. Kinetic values were obtained from these rates by Michaelis–Menten analysis using ENZFITTER software (Biosoft). Efficiency of translocation was calculated as k_{cat}/K_m, where k_{cat} is defined as V_{max}/[active site] with [active site] assumed to be the same for both ABA and ATP uptake experiments. External substrates (inhibitor, nucleotides or ABA analogues) were added to a final concentration of either 200 or 400 μM for ATP and ABA uptake experiments respectively, with either 100 nM [^{3}H]ATP or 400 nM [^{3}H]ABA respectively. Uptake was allowed to proceed for 5 min. Each point represents the average of three separate experiments.

F_1-ATPase assays

Quantification of F_1-ATPase activity was performed as described previously using an enzyme-coupled reaction and monitoring the disappearance of NADH by following absorbance at 340 nm [37,38]. F_1-ATPase assays were performed in triplicate in 200 μl volumes and were composed of 65 mM Mops/KOH (pH 8.0), 2.5 mM $MgCl_2$, 20 mM KCl, 100 μM KCN, 134 μM NADH, 25 mM $KHCO_3$ and 500 μM ATP. The reaction was initiated with the addition of 10 μg of mitochondrial preparation, 500 μM PEP (phosphoenolpyruvate), 3 units of PK (pyruvate kinase) and 2.5 units of LDH (lactate dehydrogenase), and NADH oxidation was measured at 20 °C for 30 s. Kinetic values were obtained by Michaelis–Menten analysis using ENZFITTER software (Biosoft). ABA concentration values were converted into the negative reciprocal of their log in order to plot all points of the Michaelis–Menten curve. Basal F_1-ATPase activity [recorded in the absence of (+)-ABA] was subtracted from the (+)-ABA-stimulated assays to account for any background activity. The specific ATPase inhibitors oligomycin (10 μM; [39]) and ouabain (50 μM; [40]) were applied as controls.

RESULTS AND DISCUSSION

Identification of novel putative ABA-binding proteins

Novel putative ABA-binding proteins were identified through the application of a bioactive ABA-mimetic photoactivable probe, PBI686 (Figure 1) [8,9]. In addition to a photoactivable cross-linking ABA-mimetic tetralone domain, PBI686 also contains a biotin tag. Following UV irradiation, the biotin tag allows cross-linked proteins to be detected by Western blot analysis with a streptavidin–HRP conjugate, as well as enriched by streptavidin-affinity chromatography. The aromatic ring of the tetralone in PBI686 has previously been shown to not interfere with the recognition of the compound by ABA-binding proteins [8]. Following incubation and UV irradiation of cell lysates of ABA-induced *B. napus* Jet Neuf cultures containing PBI686, cross-linked proteins were enriched by application to and elution from a streptavidin–Sepharose affinity column. Visualization of enriched fractions by Western blot analysis using a streptavidin–HRP conjugate revealed four biotin-tagged bands at ~ 65, 55, 48 and 35 kDa respectively (Figure 2, left-hand panels). The corresponding bands/regions on silver-stained gels (Figure 2, right-hand panels) were subjected to tryptic digestion and the resulting peptides were analysed by an LC-MS/MS-Q-TOF (Q-TOF is quadrupole–time-of-flight) coupled Mascot MS/MS ion search (Table 1 and Supplementary Figures S1–

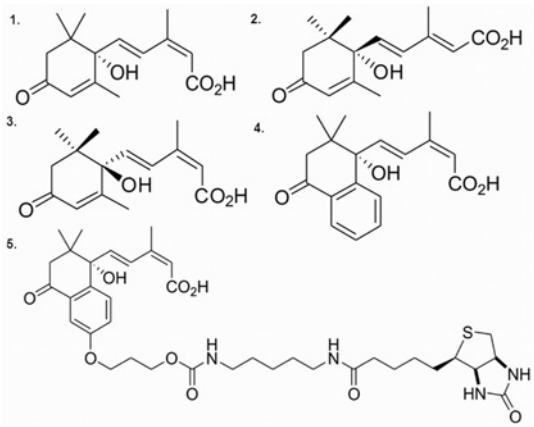

Figure 1 ABA and related ABA analogues

1, (+)-(*S*)-ABA; 2, 2-*trans*-ABA; 3, (−)-(*R*)-ABA; 4, (+)-PBI410, (+)-tetralone; 5, (+)-PBI686 photoactive, bioactive ABA-mimetic biotinylated probe used to pull-out putative ABA-binding proteins.

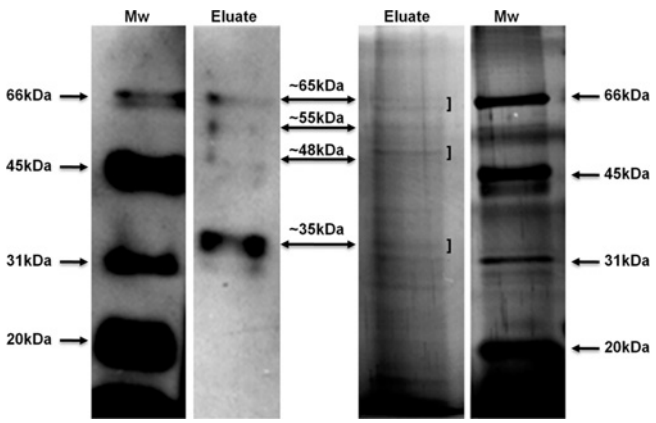

Figure 2 Streptavidin-affinity-enriched PBI686-tagged protein extracts

Total protein extract, photo-cross-linked with PBI686 was enriched using streptavidin–Sepharose affinity chromatography. Eluted proteins were desalted, concentrated and analysed using far-Western blot analysis with a streptavidin–HRP conjugate (left-hand panels) and silver-staining (right-hand panels) techniques. Band regions that were excised are indicated with a square bracket. The molecular mass in kDa is indicated.

S3 at http://www.BiochemJ.org/bj/437/bj4370117add.htm). The 65 kDa gel region was found to contain predominantly peptides homologous with the *A. thaliana* mitochondrial F_1-ATP synthase β-subunit (ATP2; At5g08690), whereas the ~48 kDa region was comprised of protein with homology with mitochondrial ANT protein. The 35 kDa region also contained peptides derived from homologues of ATP2. With an expected molecular mass of ~65 kDa, the presence of ATP2-like protein on the gel at ~35 kDa most probably represents a degradation product. These results were all shown to be reproducible. The ~55 kDa region did not yield reproducible MS data and is not addressed further in this paper.

ABA inhibits ANT-dependent ATP translocation

Mitochondrial ANTs mediate ATP/ADP exchange across the inner membranes of mitochondria (reviewed in [12]). In order to initially evaluate the relationship between ABA and ANTs, the relative effect of a 2000-fold molar excess of ATP, ABA and analogues of ABA respectively on [^{3}H]ATP

Table 1 Two putative ABA-binding proteins identified in *Brassica* cell lysates

Band/region	Protein name	NCBI/protein data	Peptides matched	Score
~65 kDa	Mitochondrial F_1-ATP synthase β-subunit	gi|17939849	8	247 (Supplementary Figure S1 at http://www.BiochemJ.org/bj/437/bj4370117add.htm)
~48 kDa	Mitochondrial ATP/ADP carrier protein	gi|944842	5	169 (Supplementary Figure S2 at http://www.BiochemJ.org/bj/437/bj4370117add.htm)
~35 kDa	Mitochondrial F_1-ATP synthase β-subunit	gi|17939849	4	179 (Supplementary Figure S3 at http://www.BiochemJ.org/bj/437/bj4370117add.htm)

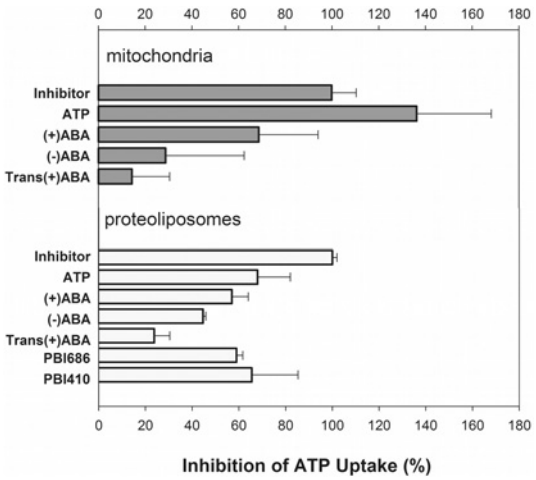

Figure 3 Inhibition of ANT-mediated ATP translocation by ABA

Effect of ATP, ABA and ABA analogues on [^{3}H]ATP uptake into mitochondria (dark grey bars). Transport was initiated by the addition of 100 nM [^{3}H]ATP to mitochondria with 200 μM substrate or 20 mM pyridoxal 5′-phosphate. Values are means $\pm$ S.D. ($n = 3$) and were plotted relative to inhibition by pyridoxal 5′-phosphate (set as 100 % inhibition). The effect of external ABA and related substrates on [^{3}H]ATP uptake in proteoliposomes (light grey bars). ANT2 proteoliposomes contained 20 mM ATP. At time zero, 100 nM [^{3}H]ATP was added with 200 μM of each of the indicated substrates. Values are means $\pm$ S.D. ($n = 4$) and are plotted relative to inhibition by pyridoxal 5′-phosphate (set as 100 % inhibition).

uptake into isolated spinach mitochondria was assessed and plotted relative to values obtained for the known ANT inhibitor pyridoxal 5′-phosphate [17,32–34,41]. ATP led to ~140 % relative inhibition (Figure 3 and Supplementary Table S1 at http://www.BiochemJ.org/bj/437/bj4370117add.htm). This observation of greater than 100 % relative inhibition is most probably explained by the presence of mitochondrial ANTs (or other translocators) in the native mitochondria that are less sensitive or insensitive to pyridoxal 5′-phosphate. (+)-ABA inhibited [^{3}H]ATP uptake by ~60 %, whereas corresponding amounts of ABA analogues, including (−)-ABA and the non-biologically relevant (+)-*trans*-ABA showed very low relative inhibition (<35 %), emphasizing specificity of the biologically relevant form. In order to address the high S.D. values and high relative inhibitions, a purified reconstituted, recombinant *A. thaliana* ANT2 proteoliposome system was subsequently applied [32]. Although S.D. values were still high in some instances, similar trends were observed (Figure 3 and Supplementary Table S2 at http://www.BiochemJ.org/bj/437/bj4370117add.htm). A 2000-fold molar excess of ATP showed the highest relative inhibition at ~70 %, with (+)-ABA showing 60 %, and related analogues showing <50 %. Although not assessed for mitochondria, PBI686 and related (+/−)-tetralone PBI410 showed relative inhibition comparable with ATP and ABA in the proteoliposome assays. Overall these results show that ABA inhibits ANT-dependent translocation of ATP and that the inhibition is relatively specific for ABA. Unsuccessful attempts at determining a simple binding constant for the purified ANT2–[^{3}H]ABA interaction suggested that the effect of ABA on ATP translocation might be the result of competition for translocation.

ABA is translocated by ANTs

Using the reconstituted ANT2 proteoliposome system, the ability of ANT2 to translocate ABA was assessed. With proteoliposomes preloaded with 20 mM (+)-ABA, external 100 nM [^{3}H]ABA was taken up, saturating at approximately 0.4 nmol of [^{3}H]ABA/g of protein, in approximately 300 s (Supplementary Figure S4 at http://www.BiochemJ.org/bj/437/bj4370117add.htm). This is comparable with values observed previously for ATP uptake in the same system (8 nmol of [^{3}H]ATP/g of protein starting with 5 μM external [^{3}H]ATP) and highlight that ANT2 can specifically translocate ABA [32]. In order to investigate biological relevance and for efficiency of preparation, we subsequently shifted back to spinach mitochondria for comparative quantification of translocation. Spinach mitochondria were used because of the intrinsically limited availability of *A. thaliana* leaf tissue for mitochondria preparation. [^{3}H]ABA (188 nM external concentration) uptake saturated at 0.3 nmol/g of protein in approximately 300 s (Figure 4A). A Michaelis–Menten analysis of rates at increasing external [^{3}H]ABA concentrations yielded a K_m of 3.5 μM and V_{max} of 2.5 nmol/min per g of protein (Figure 4B). For comparison, values for [^{3}H]ATP uptake were determined. Uptake was found to saturate at ~0.3 nmol of [^{3}H]ATP/g of protein in less than 200 s (100 nM external [^{3}H]ATP; Figure 4C), whereas a Michaelis–Menten analysis revealed a K_m of 0.4 μM and V_{max} of 1.2 nmol/min per g of protein (Figure 4D). These values for ATP uptake into mitochondria are in agreement with previously documented values [34,42], and are somewhat lower than those observed for ABA. A comparison of the efficiency of translocation (see the Experimental section for a description of this calculation), suggests that ABA is transported by mitochondrial ANTs at one-third the rate of ATP. Similarly, kinetic parameters reported for ABC transporter-catalysed ABA uptake across cell membranes (K_m values ranging from 0.25 to 1.0 μM and a V_{max} of 6.9 nmol/min per g of protein) also highlight similar kinetic values compared with ANTs [6,7]. Documented ABA concentrations inside of guard cells as high as 13 μM under stress conditions (reviewed in [43]) support the physiological relevance of the low micromolar range K_m values for ANT-dependent ABA uptake. Overall, these findings emphasize that the mechanism of ABA-mediated inhibition of ATP translocation is probably competition for translocation. At the same time, these results also raise the novel possibility that ABA may play a role inside the mitochondrial matrix.

ATP inhibits ANT-dependent ABA translocation

The specificity of [^{3}H]ABA uptake into mitochondria was assessed in the presence of a 1000-fold molar excess of externally

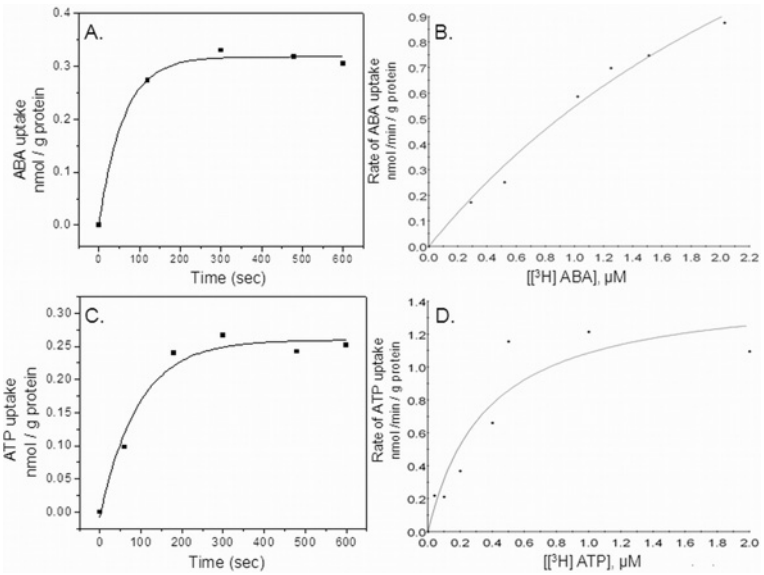

Figure 4 ABA uptake into mitochondria

(**A**) Time course of [^{3}H]ABA uptake into spinach mitochondria. Transport was initiated by adding 188 nM [^{3}H]ABA to 50 μg of mitochondria and terminated by the addition of 20 mM pyridoxal 5′-phosphate. The difference plot was obtained by the subtraction of the corresponding values for control samples pretreated with inhibitor. Each point represents mean values ($n = 5$; S.E.M. = 0.016; $R^2 = 0.991$). (**B**) Concentration-dependence of [^{3}H]ABA uptake into spinach mitochondria. Transport was initiated by adding the corresponding concentration of [^{3}H]ABA to mitochondria. Mean values are plotted for each concentration tested ($n = 5$; S.E.M. = 0.042; $R^2 = 0.986$). The kinetic values were obtained using ENZFITTER software (Biosoft). (**C**) Time-course of [^{3}H]ATP uptake into spinach mitochondria. Transport was initiated by adding 100 nM [^{3}H]ATP to mitochondria and terminated by the addition of 20 mM pyridoxal 5′-phosphate. The difference plot was obtained by subtraction of values obtained for control samples pretreated with inhibitor. Each point represents the mean ($n = 5$; S.E.M. = 0.02; $R^2 = 0.974$). (**D**) Concentration-dependence of [^{3}H]ATP uptake into spinach mitochondria. Transport was initiated by the addition of [^{3}H]ATP to mitochondria and terminated after 2 min by the addition of 20 mM pyridoxal 5′-phosphate. The difference plot was obtained by subtraction of values obtained for control samples pretreated with inhibitor. Mean values are plotted for each concentration ($n = 5$; S.E.M. = 0.0196; $R^2 = 0.974$). Kinetic values were obtained using ENZFITTER software (Biosoft).

added ATP, ABA or ABA analogues, and plotted relative to values obtained for the known ANT inhibitor, pyridoxal 5′-phosphate [17,32–34,41]. (+)-ABA inhibited uptake at a level comparable with pyridoxal 5′-phosphate, whereas ABA analogues caused only 50 % relative inhibition or less (Figure 5 and Supplementary Table S3 at http://www.BiochemJ.org/bj/437/bj4370117add.htm). (+)-*trans*-ABA showed very little effect, again emphasizing specificity of the biologically relevant form. ATP was found to be a very potent inhibitor of ABA uptake. Again to address the high S.D. values of these mitochondrial results, specificities were further probed in the ANT2-reconstituted proteoliposomes system. [^{3}H]ABA uptake was measured in the presence of a 2000-fold molar excess of an expanded repertoire of substrates. S.D. values were again still high in some instances, but similar results to those for mitochondrial uptake were obtained, supporting the general trends. (+)-ABA was found to inhibit uptake at levels comparable with pyridoxal 5′-phosphate, and ABA analogues, including PBI686 and PBI410, caused only 50 % relative inhibition or less (Figure 5 and Supplementary Table S4 at http://www.BiochemJ.org/bj/437/bj4370117add.htm). ATP and most of the other nucleotides tested were found to be very potent inhibitors of ABA uptake. The observation that UTP and GTP show the highest levels of inhibition of ABA uptake is noteworthy in that these particular nucleotides act as only very weak inhibitors of ATP translocation [32]. This opposite effect is also true for PBI686 and PBI410, shown here to be only weak inhibitors of ABA uptake and relatively strong inhibitors of ATP uptake (Figure 5). These reciprocal activity relationships suggest the possibility of differences in binding/translocation sites and/or specific mechanisms of ANT translocation for ATP and ABA. The consistently observed potency of ATP as an inhibitor of ABA uptake is in agreement with the relative efficiency of translocation of ATP compared with ABA observed in kinetic analyses.

ABA modulates mitochondrial ATPase activity

The possibility of uptake of ABA into mitochondrial matrix raises the question of the biological relevance of having ABA in the matrix. To address this, and based on the identified interaction of the PBI686 probe with the catalytic β-subunit of the F_1-ATP synthase domain (Figure 2 and Table 1), we assessed the effect of ABA on mitochondrial ATPase activity [37,38]. By way of controls, oligomycin, a H^+-ATPase-specific inhibitor was applied and found to reduce ATPase activity by ~50 %. At the same time the Na^+/K^+-ATPase-specific inhibitor ouabain was applied and found to have no effect, demonstrating that the ATPase activity measured does not arise from Na^+/K^+-driven ATPases. Upon application of ABA, a stimulation of the ATPase activity in isolated spinach mitochondrial extracts was observed, even at concentrations of ABA in the low picomolar range (Supplementary Figure S5 at http://www.BiochemJ.org/bj/437/bj4370117add.htm). However, although kinetic analysis yielded a K_a of 1.56 μM, only a 2-fold stimulation of activity was observed over the picomolar to millimolar range of ABA concentrations tested (Figure 6). Thus the K_a value is presented here only as an approximation.

In the context of an activating molecule, this limited concentration-dependent stimulation of the ATPase activity could be considered an almost negligible effect, and we do not dismiss the possibility that biologically this observed stimulation

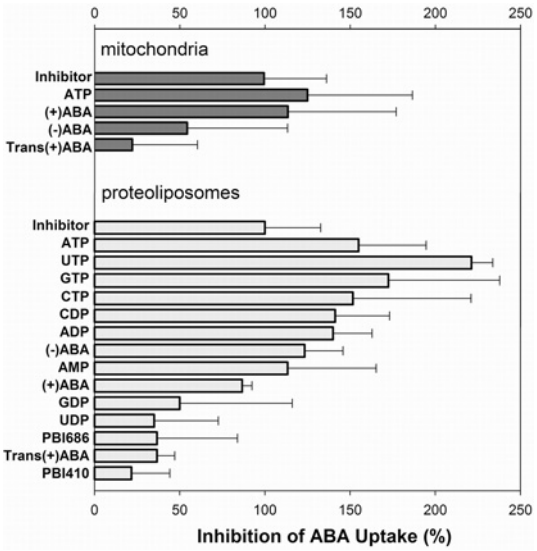

Figure 5 Specificity of ABA translocation

Effect of ATP, ABA and ABA analogues on [^{3}H]ABA uptake into mitochondria (dark grey bars). Transport was initiated by the addition of 400 nM [^{3}H]ABA added together with 400 μM substrates or 20 mM pyridoxal 5′-phosphate. Values represent means + S.D. ($n = 3$). Values were plotted relative to inhibition by pyridoxal 5′-phosphate (set as 100 % inhibition). The effect of ATP and ABA and their related analogues on [^{3}H]ABA uptake into proteoliposomes is shown as light grey bars. ANT2 proteoliposomes contained 20 mM ABA. Transport was terminated after 10 min. External substrates were added (final concentration 2.5 mM each) together with [^{3}H]ABA (100 nM). Values are means + S.D. ($n = 4$), and were plotted relative to inhibition by pyridoxal 5′-phosphate (set as 100 % inhibition).

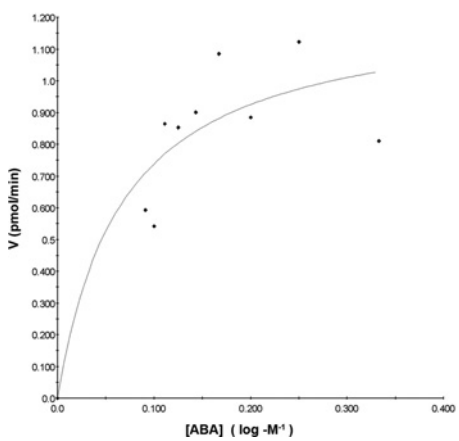

Figure 6 ABA modulation of F_1-ATPase activity in mitochondrial extracts

Purified spinach mitochondrial extracts were assayed for F_1-ATPase activity in the presence of increasing concentrations of ABA ($n = 3$). Basal activity in the absence of ABA was substracted at all time points assayed to obtain activation rates for each ABA concentration tested. Michaelis–Menten analysis was used to evaluate the K_a of F_1-ATPase for ABA over concentrations ranging from picomolar to millimolar. ABA concentrations were plotted as the negative reciprocal of their logarithm.

of ATPase is not relevant, or only of secondary importance to the effect of ABA on modulation of ATP translocation. However, energetically, a 2-fold increase in ATPase activity is fairly significant, and this stimulation is observed even at low picomolar concentrations of ABA. Physiologically, cytosolic ABA concentrations transiently reach a maximum of approximately 5–10 μM under stress conditions, which correlates with the K_m of 3.5 μM determined for ABA translocation into mitochondria. More speculatively, taking the demonstrated relative specificity of the ANTs for ABA and ATP into consideration, concentrations of ABA accumulating in the mitochondrial matrix would not probably be very high; potentially in the order of picomolar to nanomolar at best, correlating with the effect of picomolar concentrations of ABA on ATPase activity described above. In further support of the general concept of ABA modulating membrane pumps, the β-subunit of the chloroplast ATP synthase complex was also recently identified, although not characterized, as a putative ABA-binding protein [9]. At the same time, other reports have shown that ABA induces depolarization of the plasma membrane via the inhibition of the plasma membrane pumps in *A. thaliana* cell culture [44]. It was also shown that ABA has direct and indirect effects on plasma membrane and vacuolar H^+-ATPases in response to salt stress [45,46]. Overall, although not conclusive regarding biological relevance, the ABA-dependent ATPase stimulation demonstrated in the present study does validate the initial interaction observed in the pull-down of F_1-ATP synthase β-subunit using PBI686, and suggests one possibility for a role for ABA inside the mitochondria.

The work described in the present study was completed entirely *in vitro* specifically to preclude the possibility of competing gene regulation effects. Indeed two previous reports highlight gene regulation as an important mechanism of ABA action related to mitochondrial modulation. In one instance ABA was shown to stimulate mitochondrial activity through induction of the expression of antioxidant enzymes, whereas the second study highlights ABA gene induction of mitochondrial ANT1 [15,16]. Less relevant, but in the same vein, a third study showed ABA to significantly increase expression of chloroplast ATP-synthase CF_1 α-subunit [38]. Taking these previous studies [15,16,38] and the findings of the present study together, we conclude that ABA potentially regulates mitochondrial functionality through a number of different mechanisms including gene regulation, as well as mechanisms based on direct interaction of ABA with ANTs and possibly mitochondrial matrix-localized proteins.

Conclusion

In conclusion, the *in vitro* results of the present study highlight novel interactions between ABA and mitochondrial proteins, suggesting the possibility of an as yet uncharacterized mechanism of ABA action *in planta*. Whether the translocation of ABA by ANTs is primarily directed at inhibiting ATP translocation, or towards enabling interactions with mitochondrial matrix-localized proteins, or both, remains to be determined.

AUTHOR CONTRIBUTION

Olesya Kharenko designed and performed the ANT related experiments, analysed the data and wrote the paper. Jason Boyd designed and performed the ATPase-related experiments and analysed the data. Ken Nelson synthesized and purified all ABA and related analogues. Suzanne Abrams conceived the idea. Michele Loewen designed experiments, analysed and interpreted the data, and wrote the paper.

ACKNOWLEDGEMENTS

We thank Dr Andrew Ross and the Mass Spectroscopy facility of the National Research Council for MS analysis, Dr Michelle Alting-Meese and Dr Marek Galka for discussions and Dr Peter Loewen (University of Manitoba), Dr Pierre Fobert and Dr Adrian Cutler (Plant Biotechnology Institute/National Research Council Canada) for critical reading of the manuscript prior to submission. This manuscript represents NRCC# 50170.

FUNDING

This work was suppported by a National Research Council of Canada – Genomics Health Initiative grant to M.C.L and S.R.A.

REFERENCES

1 Smet, I. D., Zhang, H., Inze, D. and Beeckman, T. (2006) A novel role for abscisic acid emerges from underground. Trends Plant Sci. **11**, 434–439
2 Ma, Y., Szostkiewicz, I., Korte, A., Moes, D., Yang, Y., Christmann, A. and Grill, E. (2009) Regulators of PP2C phosphatase activity function as abscisic acid sensors. Science **324**, 1064–1068
3 Park, S.-Y., Fung, P., Nishimura, N., Jensen, D. R., Fujii, H., Zhao, Y., Lumba, S., Santiago, J., Rodrigues, A., Chow, T.-f. F. et al. (2009) Abscisic acid inhibits type 2C protein phosphatases via the PYR/PYL family of START proteins. Science **324**, 1068–1071
4 Pandey, S., Nelson, D. C. and Assmann, S. M. (2009) Two novel GPCR-type G proteins are abscisic acid receptors in *Arabidopsis*. Cell **136**, 136–148
5 Shang, Y., Yan, L., Liu, Z.-Q., Cao, Z., Mei, C., Xin, Q., Wu, F.-Q., Wang, X.-F., Du, S.-Y., Jiang, T. et al. (2010) The Mg-chelatase H subunit of *Arabidopsis* antagonizes a group of transcription repressors to relieve ABA-responsive genes of inhibition. Plant Cell **22**, 1909–1935
6 Kang, J., Hwang, J.-U., Lee, M., Kim, Y.-Y., Assmann, S. M., Martinoia, E. and Lee, Y. (2010) PDR-type ABC transporter mediates cellular uptake of the phytohormone abscisic acid. Proc. Natl. Acad. Sci. U.S.A. **107**, 2355–2360
7 Kuromori, T., Miyaji, T., Yabuuchi, H., Shimizu, H., Sugimoto, E., Kamiya, A., Moriyama, Y. and Shinozaki, K. (2010) ABC transporter AtABCG25 is involved in abscisic acid transport and responses. Proc. Natl. Acad. Sci. U.S.A. **107**, 2361–2366
8 Nyangulu, J. M., Galka, M. M., Jadhav, A., Gai, Y., Graham, C. M., Nelson, K. M., Cutler, A. J., Taylor, D. C., Banowetz, G. M. and Abrams, S. R. (2005) An affinity probe for isolation of abscisic acid-binding proteins. J. Am. Chem. Soc. **127**, 1662–1664
9 Galka, M. M. (2009) Identification of abscisic acid binding proteins using a bioactive photoaffinity probe, Ph.D. Thesis, University of Saskatchewan, Saskatoon, Canada
10 Devenish, R. J., Prescott, M. and Rodgers, A. J. (2008) The structure and function of mitochondrial F_1F_0-ATP synthases. Int. Rev. Cell. Mol. Biol. **267**, 1–58
11 Pedersen, P. L. (2007) Transport ATPases into the year 2008: a brief overview related to types, structures, functions and roles in health and disease. J. Bioenerg. Biomembr. **39**, 349–355
12 Klingenberg, M. (2008) The ADP and ATP transport in mitochondria and its carrier. Biochim. Biophys. Acta **1778**, 1978–2021
13 Nury, H., Dahout-Gonzalez, C., Trezeguet, V., Lauquin, G. J., Brandolin, G. and Pebay-Peyroula, E. (2006) Relations between structure and function of the mitochondrial ADP/ATP carrier. Annu. Rev. Biochem. **75**, 713–741
14 Neuhaus, H. E., Thom, E., Mohlmann, T., Steup, M. and Kampfenkel, K. (1997) Characterization of a novel eukaryotic ATP/ADP translocator located in the plastid envelope of *Arabidopsis thaliana* L. Plant J. **11**, 73–82
15 Prasad, T. K., Anderson, M. D. and Stewart, C. R. (1994) Acclimation, hydrogen peroxide, and abscisic acid protect mitochondria against irreversible chilling injury in maize seedlings. Plant Physiol. **105**, 619–627
16 Millar, A. H. and Heazlewood, J. L. (2003) Genomic and proteomic analysis of mitochondrial carrier proteins in *Arabidopsis*. Plant Physiol. **131**, 443–453
17 Palmieri, L., Santoro, A., Carrari, F., Blanco, E., Nunes-Nesi, A., Arrigoni, R., Genchi, F., Fernie, A. R. and Palmieri, F. (2008) Identification and characterization of ADNT1, a novel mitochondrial adenine nucleotide transporter from *Arabidopsis*. Plant Physiol. **148**, 1797–1808
18 Pastore, D., Trono, S., Laus, M. N., Fonzo, M. D. and Flagella, Z. (2007) Possible plant mitochondria involvement in cell adaptation to drought stress. J. Exp. Bot. **58**, 195–210
19 Kaklewski, K., Nowak, J. and Ligocki, M. (2008) Effects of selenium content in green parts of plants on the amount of ATP and ascorbate-glutathione cycle enzyme activity at various growth stages of wheat and oilseed rape. J. Plant Physiol. **165**, 1011–1022
20 Kim, S.-H., Yang, S. H., Kim, T.-J., Han, J.-S. and Suh, J.-W. (2009) Hypertonic stress increased extracellular ATP levels and the expression of stress-responsive genes in *Arabidopsis thaliana* seedlings. Biosci. Biotech. Biochem. **73**, 1252–1256
21 Sobczyk, E. and Kacperska-Palacz, A. (1979) Adenine nucleotide changes during cold acclimation of winter rape plants. Plant Physiol. **62**, 875–878
22 Song, C. J., Steinebrunner, I., Wang, X., Stout, S. C. and Roux, S. J. (2006) Extracellular ATP induces the accumulation of superoxide via NADPH oxidases in *Arabidopsis*. Plant Physiol. **140**, 1222–1232
23 Sweetlove, L. J., Heazlewood, J. L., Herald, V., Holtzapffel, R., Day, D. A., Leaver, C. J. and Millar, A. H. (2002) The impact of oxidative stress on *Arabidopsis* mitochondria. Plant J. **32**, 891–904
24 Zhang, X., Takano, T. and Liu, S. (2006) Identification of a mitochondrial ATP synthase small subunit gene (RMtATP6) expressed in response to salts and osmotic stresses in rice (*Oryza sativa* L.). J. Exp. Bot. **57**, 193–200
25 Hamilton, C. A., Good, A. G. and Taylor, G. J. (2001) Induction of vacuolar ATPase and mitochondrial ATP synthase by aluminum in an aluminum-resistant cultivar of wheat. Plant Physiol. **125**, 2068–2077
26 Abrams, S. R., Reaney, M. J. T., Abrams, G. D., Mazurek, T., Shaw, A. C. and Gusta, L. V. (1989) Ratio of (*S*)- to (*R*)-abscisic acid from plant cell cultures supplied with racemic ABA. Phytochemistry **28**, 2885–2889
27 Nyangulu, J. M., Nelson, K. M., Rose, P. A., Gai, Y., Loewen, M., Lougheed, B., Quail, J. W., Cutler, A. J. and Abrams, S. R. (2006) Synthesis and biological activity of tetralone abscisic acid analogues. Org. Biomol. Chem. **4**, 1400–1412
28 Lichter, R. (1981) Anther culture of *Brassica napus* in a liquid medium. Z. Pflanzenphysiol. **103**, 229–237
29 Weselake, R., Byers, S., Davoren, J., Laroche, A., Hodges, D., Pomeroy, M. and Furukawa-Stoffer, T. (1998) Triacylglycerol biosynthesis and gene expression in microspore-derived cell suspension cultures of oilseed rape. J. Exp. Bot. **49**, 33–39
30 Laemmli, U. K. (1970) Cleavage of structural proteins during the assembly of the head of bacteriophage T4. Nature **227**, 680–685
31 Sheoran, I. S., Olson, D. J., Ross, A. R. and Sawhney, V. K. (2005) Proteome analysis of embryo and endosperm from germinating tomato seeds. Proteomics **5**, 3752–3764
32 Kharenko, O. A. and Loewen, M. C. (2010) Characterization of the ATP-translocating properties of the predicted *Arabidopsis thaliana* mitochondrial adenine nucleotide translocator 2. Botany **88**, 685–690
33 Genchi, G., Ponzone, C., Bisaccia, F., De Santis, A., Stefanizzi, L. and Palmieri, F. (1996) Purification and characterization of the reconstitutively active adenine nucleotide carrier from maize mitochondria. Plant Physiol. **112**, 845–851
34 Thuswaldner, S., Lagerstedt, J. O., Rojas-Stutz, M., Bouhidel, K., Der, C., Leborgne-Castel, N., Mishra, A., Marty, F., Schoefs, B., Adamska, I. et al. (2007) Identification, expression, and functional analyses of a thylakoid ATP/ADP carrier from *Arabidopsis*. J. Biol. Chem. **282**, 8848–8859
35 Hamasur, B., Birgersson, U., Eriksson, A. and Glaser, E. (1990) Large-scale purification procedure of spinach leaf mitochondria: isolation and immunological studies of the F1-ATPase. Physiol. Plant. **78**, 367–373
36 LaNoue, K. F. and Schoolwerth, A. C. (1979) Metabolite transport in mitochondria. Annu. Rev. Biochem. **48**, 871–922
37 Fisher, R. J., Liang, A. M. and Sundstrom, G. C. (1981) Selective disaggregation of the H^+-translocating ATPase. Isolation of two discrete complexes of the rutamycin-insensitive ATPase differing in mitochondrial membrane-binding properties. J. Biol. Chem. **256**, 707–715
38 Zhu, M., Simons, B., Zhu, N., Oppenheimer, D. G. and Chen, S. (2010) Analysis of abscisic acid responsive proteins in *Brassica napus* guard cells by multiplexed isobaric tagging. J. Proteomics **73**, 790–805
39 Devenish, R. J., Prescott, M., Boyle, G. M. and Nagley, P. (2000) The oligomycin axis of mitochondrial ATP synthase: OSCP and the proton channel. J. Bioenerg. Biomembr. **32**, 507–515
40 Lingrel, J. B. (2010) The physiological significance of the cardiotonic steroid/ouabain-binding site of the Na,K-ATPase. Annu. Rev. Physiol. **72**, 395–412
41 Bogner, W., Aquila, H. and Klingenberg, M. (1986) The transmembrane arrangement of the ADP/ATP carrier as elucidated by the lysine reagent pyridoxal 5-phosphate. J. Biol. Chem. **161**, 611–620
42 Weidemann, M. J., Erdelt, H. and Klingenberg, M. (1970) Adenine nucleotide translocation of mitochondria: identification of carrier sites. Eur. J. Biochem. **16**, 313–335
43 McCourt, P. and Creelman, R. (2008) The ABA receptors: we report you decide. Curr. Opin. Plant Biol. **11**, 474–478
44 Brault, M., Zmiar, Z., Pennarun, A.-M., Monestiez, M., Zhang, Z., Cornel, D., Dellis, O., Knight, H., Bouteau, F. and Rona, J.-P. (2004) Plasma membrane depolarization induced by abscisic acid in *Arabidopsis* suspension cells involves reduction of proton pumping in addition to anion chanel activation, which are both Ca^{2+}-dependent. Plant Physiol. **135**, 231–243
45 Fukuda, A. and Tanaka, Y. (2006) Effects of ABA, auxin, and gibberellin on the expression of genes for vacuolar H^+-inorganic pyrophosphatase, H^+-ATPase subunit A, and Na^+/H^+ antiporter in barley. Plant Phys. Biochem. **44**, 351–358
46 Janica-Russak, M. and Klobus, G. (2007) Modification of plasma membrane and vacuolar H^+-ATPase in response to NaCl and ABA. J. Plant Phys. **164**, 295–302

Received 17 November 2010/17 March 2011; accepted 7 April 2011
Published as BJ Immediate Publication 7 April 2011, doi:10.1042/BJ20101898

Biochem. J. (2011) **437**, 117–123 (Printed in Great Britain) doi:10.1042/BJ20101898

online data

SUPPLEMENTARY ONLINE DATA

Identification and characterization of interactions between abscisic acid and mitochondrial adenine nucleotide translocators

Olesya A. KHARENKO*, Jason BOYD*, Ken M. NELSON*, Suzanne R. ABRAMS*† and Michele C. LOEWEN*‡[1]

*Plant Biotechnology Institute, National Research Council of Canada, 110 Gymnasium Place, Saskatoon, SK, Canada S7N 0W9, †Department of Chemistry, University of Saskatchewan, 110 Science Place, Saskatoon, SK, Canada S7N 5C9, and ‡Department of Biochemistry, 107 Wiggins Road, Saskatoon SK, Canada S7N 5E5

gi|17939849. Mass: 53288 Score: 247 Peptides matched: 8 mitochondrial F1 ATP synthase beta subunit [*Arabidopsis thaliana*]

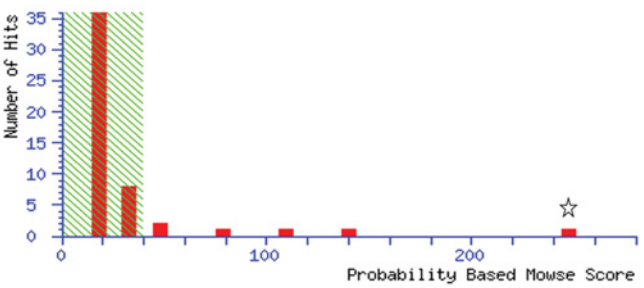

Query	Observed	Mr(expt)	Mr(calc)	Delta	Miss	Score	Expect	Rank	Peptide
4	402.19	802.36	802.35	0.01	0	12	43	2	K.TYDYGGK.G
☑ 23	433.70	865.39	865.39	0.00	0	47	0.0085	1	R.EGNDLYR.E
41	503.27	1004.52	1004.52	0.00	0	15	16	6	R.EMIESGVIK.L
☑ 44	511.28	1020.54	1020.52	0.03	0	(15)	30	1	R.EMIESGVIK.L + Oxidation (M)
☑ 60	587.33	1172.65	1172.66	-0.00	0	38	0.069	1	K.VVDLLAPYQR.G
☑ 70	639.82	1277.63	1277.63	0.00	0	46	0.012	1	R.TIAMDGTEGLVR.G + Oxidation (M)
☑ 74	697.42	1392.82	1392.81	0.01	0	36	0.14	1	K.VLNTGAPITVPVGR.A
☑ 75	701.36	1400.70	1400.70	0.00	0	57	0.0012	1	R.IMNVLGEPIDER.G + Oxidation (M)

Figure S1 MS/MS ion search results (Mascot) of the digested ~65 kDa gel region

Protein fractions were eluted by streptavidin–Sepharose affinity columns, desalted, concentrated using Amicon™ Ultrafree centrifugal filters (Millipore), and visualized using a FOCUS-FAST silver-stain kit. The ~65 kDa band/region was excised and analysed by LC-MS/MS and Mascot ion search methods as described in the Experimental section of the main paper.

gi|944842 Mass: 36013 Score: 169 Peptides matched: 5 ATP/ADP carrier protein [*Triticum turgidum*]

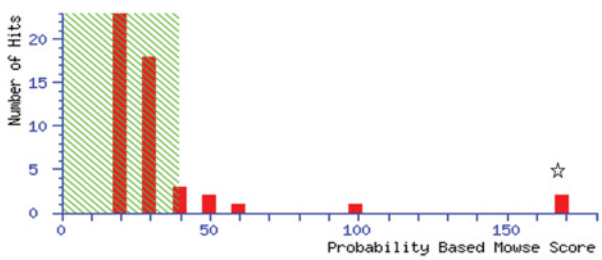

Query	Observed	Mr(expt)	Mr(calc)	Delta	Miss	Score	Expect	Rank	Peptide
☑ 10	414.73	827.44	827.45	-0.01	0	58	0.00062	1	K.TAAAPIER.V
☑ 21	422.74	843.46	843.46	-0.00	0	36	0.13	1	R.GNTANVIR.Y
☑ 37	441.22	880.42	880.39	0.03	0	19	5.3	1	K.GIGDCFGR.T
☑ 46	476.25	950.48	950.48	-0.00	0	17	8.4	1	K.SDGIAGLYR.G
☑ 110	680.87	1359.72	1359.71	0.01	0	38	0.063	1	K.LLIQNQDEMIK.A + Oxidation (M)

Figure S2 MS/MS ion search results (Mascot) of the digested ~48 kDa gel region

Protein fractions were eluted by streptavidin–Sepharose affinity columns, desalted, concentrated using Amicon™ Ultrafree centrifugal filters (Millipore), and visualized using a FOCUS-FAST silver-stain kit. The ~48 kDa band/region was excised and analysed by LC-MS/MS and Mascot ion search methods as described in the Experimental section of the main paper.

[1] To whom correspondence should be addressed (email michele.loewen@nrc.ca).

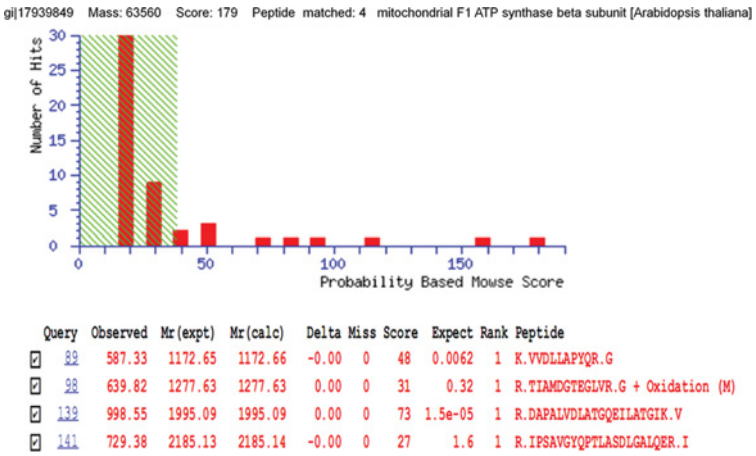

Query	Observed	Mr(expt)	Mr(calc)	Delta	Miss	Score	Expect	Rank	Peptide
89	587.33	1172.65	1172.66	-0.00	0	48	0.0062	1	K.VVDLLAPYQR.G
98	639.82	1277.63	1277.63	0.00	0	31	0.32	1	R.TIAMDGTEGLVR.G + Oxidation (M)
139	998.55	1995.09	1995.09	0.00	0	73	1.5e-05	1	R.DAPALVDLATGQEILATGIK.V
141	729.38	2185.13	2185.14	-0.00	0	27	1.6	1	R.IPSAVGYQPTLASDLGALQER.I

Figure S3 MS/MS ion search results (Mascot) of the digested ~35 kDa gel region

Protein fractions were eluted by streptavidin–Sepharose affinity columns, desalted, concentrated using Amicon™ Ultrafree centrifugal filters (Millipore), and visualized using a FOCUS-FAST silver-stain kit. The ~35 kDa band/region was excised and analysed by LC-MS/MS and Mascot ion search methods as described in the Experimental section of the main paper.

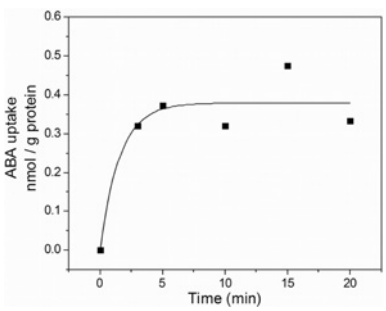

Figure S4 Time course of ABA uptake into proteoliposomes

ANT2-reconstituted proteoliposomes contained 20 mM ABA. Transport was initiated by the addition of 100 nM [^{3}H]ABA at time zero and terminated by the addition of 2.0 mM pyridoxal 5′-phosphate inhibitor at the indicated time points. Data points, means ($n = 6$), were calculated by subtracting values obtained for control samples pretreated with inhibitor.

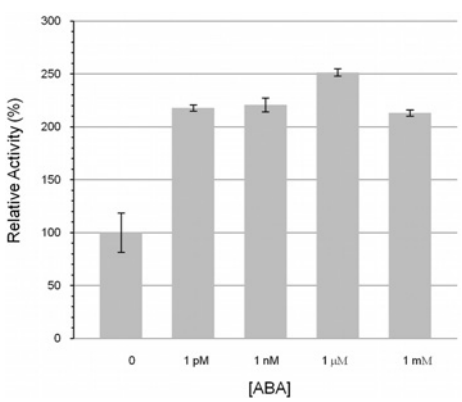

Figure S5 Relative F_1-ATPase activity in the absence and presence of various concentrations of (+)-ABA

Spinach mitochondrial extracts assayed for relative F_1-ATPase activity using standard conditions including 500 μM ATP and 134 μM NADH with the addition of (+)-ABA over a concentration range of 0, 1 pM, 1 nM, 1 μM and 1 mM. Mean values with S.D. ($n = 3$).

Table S1 Sensitivity of mitochondrial ATP uptake to externally added substrates

Transport was initiated by the addition of 100 nM [^{3}H]ABA to mitochondria with 200 μM substrate or 20 mM pyridoxal 5′- phosphate. Values are means ± S.D. ($n = 3$).

External substrate	Percentage inhibition
Pyridoxal 5′-phosphate	44 ± 4.6
ATP	65 ± 9.7
(+)-ABA	30 ± 11.2
(−)-ABA	13 ± 14.8
(+)-*trans*-ABA	6 ± 6.7

Table S2 Sensitivity of ANT2 proteoliposome ATP/ATP exchange to externally added substrates

ANT2 proteoliposomes contained 20 mM ATP. At time zero 100 nM [^{3}H]ATP was added with 200 μM of each of the indicated substrates. Values are means ± S.D. ($n = 4$).

External substrate	Percentage inhibition
Pyridoxal 5′-phosphate	30 ± 0.6
ATP	23 ± 4.6
(+)-ABA	17 ± 2.1
(−)-ABA	14 ± 0.4
(+)-*trans*-ABA	7 ± 2
PBI686	18 ± 0.78
PBI410	20 ± 5.3

Table S3 Sensitivity of mitochondrial ABA uptake to externally added substrates

Transport was initiated by the addition of 400 nM [^{3}H]ABA added together with 400 μM substrates or 20 mM pyridoxal 5′- phosphate. Values are means ± S.D. ($n = 3$).

External substrate	Percentage inhibition
Pyridoxal 5′-phosphate	20 ± 7.2
ATP	25 ± 12.1
(+)-ABA	22 ± 12.5
(−)-ABA	11 ± 11.5
(+)-*trans*-ABA	4 ± 7.5

Received 17 November 2010/17 March 2011; accepted 7 April 2011
Published as BJ Immediate Publication 7 April 2011, doi:10.1042/BJ20101898

Table S4 Sensitivity of ABA/ABA exchange in proteoliposomes to externally added substrates

ANT2 proteoliposomes contained 20 mM ABA. Transport was terminated after 10 min. External substrates were added (final concentration 2.5 mM each) together with [^{3}H]ABA (100 nM). Values are means ± S.D. (n=4).

External substrate	Percentage inhibition
Pyridoxal 5′-phosphate	20 ± 6.6
ATP	31 ± 7.9
UTP	44 ± 2.5
GTP	35 ± 13.1
CTP	30 ± 13.9
CDP	28 ± 6.4
ADP	28 ± 4.6
(−)-ABA	25 ± 4.5
AMP	23 ± 10
(+)-ABA	17 ± 1.2
GDP	10 ± 13.2
UDP	7 ± 7.5
PBI686	7 ± 9.5
(+)-*trans*-ABA	7 ± 2.1
PBI410	4 ± 4.5